C−H Activation of Substituted Arenes by Tungsten Alkylidene Complexes: Products, Selectivity, and Mechanism

Craig S. Adams, Peter Legzdins,* and Elizabeth Tran

Department of Chemistry, The University of British Columbia, Vancouver, British Columbia, Canada V6T 1Z1

Received November 19, 2001

Thermolyses (70 °C, 40 h) of Cp*W(NO)(CH_2CMe_3)$_2$ (**1**) and Cp*W(NO)(CH_2CMe_3)($CH_2C_6H_5$) (**2**) in xylenes, mesitylene, and α,α,α-trifluorotoluene generate mixtures of the corresponding aryl and/or benzyl products derived from aromatic sp^2 and benzylic sp^3 C−H bond activations of the solvent molecules by the intermediate alkylidene complexes Cp*W(NO)(=CHCMe$_3$)(σ-CMe$_4$) (σ-**A**) and Cp*W(NO)(=CHC$_6$H$_5$)(σ-CMe$_4$) (σ-**B**), respectively. For instance, the thermolysis of **1** in *p*-xylene affords products resulting from the activation of one and two molecules of *p*-xylene. The two products derived from the activation of one solvent molecule are Cp*W(NO)(CH_2CMe_3)(C_6H_3-2,5-Me$_2$) (**10**) and Cp*W(NO)(CH_2CMe_3)($CH_2C_6H_4$-4-Me) (**11**). The other two complexes derived from the activation of two solvent molecules are Cp*W(NO)($CH_2C_6H_4$-4-Me)(C_6H_4-2,5-Me$_2$) (**12**) and Cp*W(NO)($CH_2C_6H_4$-4-Me)$_2$ (**13**). The ratio of the four products in the final reaction mixture is **10**:**11**:**12**:**13** = 1.81 ± 0.09:0.44 ± 0.05:1.0:0.15 ± 0.02. All new complexes prepared have been characterized as fully as possible by conventional spectroscopic methods, and the solid-state molecular structures of Cp*W(NO)($CH_2C_6H_5$)(C_6H_3-2,5-Me$_2$) (**7**) and Cp*W(NO)($CH_2C_6H_5$)($CH_2C_6H_3$-3,5-Me$_2$) (**9**) have been established by X-ray diffraction methods. Analyses of the product distributions resulting from the various thermolyses indicate that the benzyl products are increasingly favored over the aryl products as the number of methyl substituents on the solvent molecule increases. Likewise, the movement of the methyl groups from the ortho to meta to para position in the xylenes shifts the aryl vs benzyl product distribution toward the benzyl products. With respect to the aryl product regioselectivities, only the least sterically congested aryl regioisomers are formed in the activations of *o*- and *m*-xylene, while the meta and para aryl products are formed preferentially for α,α,α-trifluorotoluene. Finally, the distributions obtained from σ-**B** are more abundant in the aryl products than are those obtained from σ-**A**. However, despite these general trends, it is also apparent that the origin of the observed product selectivities is highly dependent on the nature of the substrate, the nature of the C−H activation products, and the intermediate alkylidene complex.

Introduction

The activation and functionalization of hydrocarbons continues to be a matter of both academic and industrial interest.[1,2] One branch of the ongoing research in this area concerns the development and understanding of metal-based systems that activate the C−H bonds of hydrocarbons to yield products with new metal−carbon bonds.[3,4] An advantage of these organometallic C−H activation systems is that the product selectivities are typically opposite those exhibited by radical and electrophilic C−H activation processes.[4] A wide variety of metal complexes is now known to effect selective organometallic hydrocarbon C−H bond activations via several different mechanisms.[5,6,7]

In recent years we have been investigating a rare mode of intermolecular hydrocarbon C−H activation in which the substrate C−H bond scission occurs via addition across the M=C linkage of an alkylidene complex.[8−10] As summarized in Scheme 1, we have to date established that in solutions at 70 °C the complexes

(1) Shilov, A. E.; Shul'pin, G. B. *Activation and Catalytic Reactions of Saturated Hydrocarbons in the Presence of Metal Complexes*; Kluwer Academic Publishers: Norwell, MA, 2000.
(2) Crabtree, R. H. *Chem. Rev.* **1995**, *95*, 987−1007.
(3) For a recent review of the field, see: Crabtree, R. H. *J. Chem. Soc., Dalton Trans.* **2001**, 2437−2450.
(4) For other leading reviews, see: (a) Arndtsen, B. A.; Bergman, R. G.; Mobley, T. A.; Peterson, T. H. *Acc. Chem. Res.* **1995**, *28*, 154−162. (b) Sen, A. *Acc. Chem. Res.* **1998**, *31*, 550−557. (c) Stahl, S. S.; Labinger, J. A.; Bercaw, J. E. *Angew. Chem., Int. Ed.* **1998**, *37*, 2180−2192. (d) *Activation and Functionalization of Alkanes*; Hill, C. L., Ed.; Wiley-Interscience: New York, 1989.
(5) Peterson, T. H.; Golden, J. T.; Bergman, R. G. *J. Am. Chem. Soc.* **2001**, *123*, 455−462, and references therein.
(6) (a) Erker, G. *J. Organomet. Chem.*, **1977**, *134*, 189−202. (b) Watson, P. L.; Parshall, G. W. *Acc. Chem. Res.* **1985**, *18*, 51−56. (c) Fendrick, C. M.; Marks, T. J. *J. Am. Chem. Soc.* **1986**, *108*, 425−437. (d) Thompson, M. E.; Baxter, S. M.; Bulls, R.; Burger, B. J.; Nolan, M. C.; Santarsiero, B. D.; Schaefer, W. P.; Bercaw, J. E. *J. Am. Chem. Soc.* **1987**, *109*, 203−219. (e) Debad, J. D.; Legzdins, P.; Lumb, S. A.; Rettig, S. J.; Batchelor, R. J.; Einstein, F. W. B. *Organometallics* **1999**, *18*, 3414−3428.
(7) Schaefer, D. F., II; Wolczanski, P. T. *J. Am. Chem. Soc.* **1998**, *120*, 4881−4882 and references therein.
(8) Tran, E.; Legzdins, P. *J. Am. Chem. Soc.* **1997**, *119*, 5071−5072.
(9) Adams, C. S.; Legzdins, P.; Tran, E. *J. Am. Chem. Soc.* **2001**, *123*, 612−624.

10.1021/om011000q CCC: $22.00
Publication on Web 03/05/2002

Scheme 1

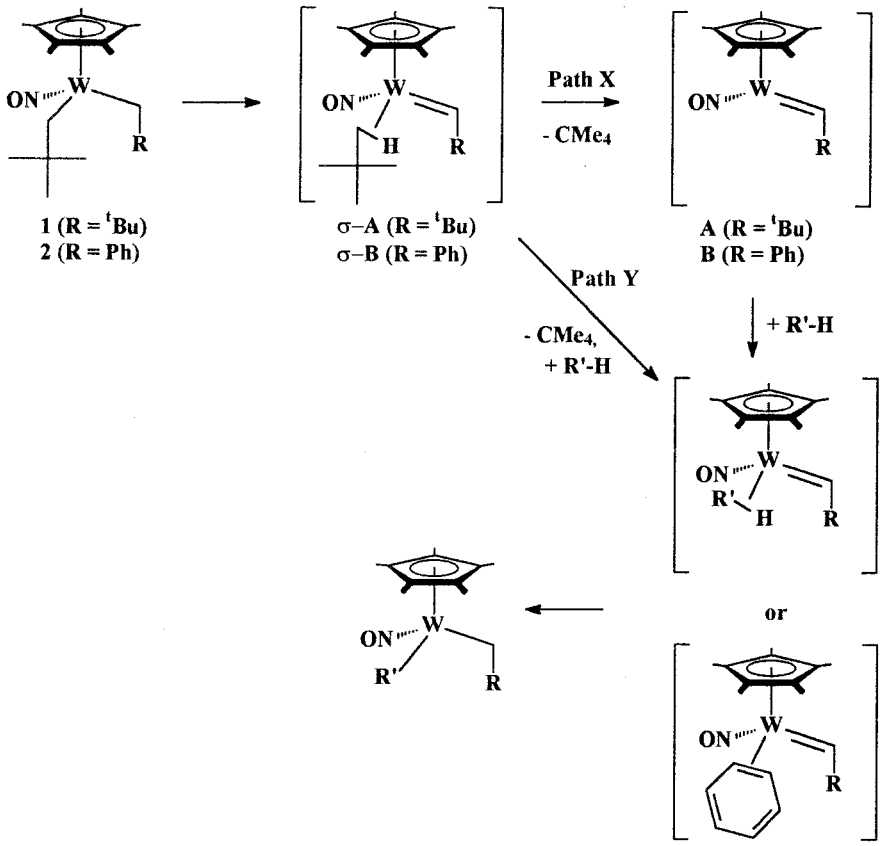

$Cp^*W(NO)(CH_2CMe_3)_2$ (**1**) and $Cp^*W(NO)(CH_2CMe_3)(CH_2C_6H_5)$ (**2**) generate, at equivalent rates via rate-determining α-H abstraction, the respective alkylidene σ-neopentane complexes, namely, $Cp^*W(NO)(=CHCMe_3)(\sigma\text{-}CMe_4)$ (σ-**A**) and $Cp^*W(NO)(=CHC_6H_5)(\sigma\text{-}CMe_4)$ (σ-**B**).[10] These intermediates then lose neopentane and either generate the 16e alkylidene complexes $Cp^*W(NO)(=CHCMe_3)$ (**A**) and $Cp^*W(NO)(=CHC_6H_5)$ (**B**) as discrete intermediates (path X, Scheme 1) or react directly with a molecule of hydrocarbon solvent (R′−H) (path Y, Scheme 1). The activation of alkane or arene substrates by either reactive species then proceeds by formation of intermediate hydrocarbon complexes, either σ-complexes for alkane and benzylic sp^3 C−H bonds or π-arene complexes for aromatic sp^2 bonds, followed by C−H bond scission. For simplicity and brevity, the reactive neopentylidene and benzylidene species shown in Figure 1 are considered to be σ-**A** and σ-**B**, respectively, throughout this report. However, it should be understood that parallel rationales and explanations involving **A** and **B** are also valid.[11] In any event, these tungsten alkylidene complexes are the only such systems reported to date that activate both alkane and arene substrates to form isolable organometallic products.[12]

We have previously studied the activation of toluene by these alkylidene complexes and have discovered several interesting features.[9,10] Specifically, we have found that the thermolyses of **1** and **2** in this solvent generate mixtures of the respective aryl and benzyl products derived from aromatic sp^2 and benzylic sp^3 C−H bond activations.[9] In the case of **1**, complex **2** is generated in situ from benzylic sp^3 bond activation, and so products derived from the activation of toluene by both σ-**A** and σ-**B** are present in the final reaction mixture. During the activations mediated by the two alkylidene species, the aryl products, in particular the meta and para isomers, are formed preferentially over the benzyl products. Specifically, the distributions obtained from σ-**B** are much richer in aryl products, in particular the meta regioisomers.[13]

Additional experimental data indicate that the aryl and benzyl products are formed irreversibly via separate pathways, but that the aryl regioisomers undergo rapid isomerization via reversible aromatic sp^2 C−H bond scission under the thermolytic conditions (Scheme 2).[10] Hence, for toluene, the aryl vs benzyl product selectivity is under kinetic control and is governed by the relative rates of formation of the respective π-arene and σ-phenylmethane complexes from the reactive alkylidene species ($\Delta\Delta G^{\ddagger}$ in Figure 1).[10] In contrast, the ortho vs meta vs para aryl regioselectivity is under thermodynamic control and is determined by the relative energies of the ortho, meta, and para aryl products ($\Delta\Delta G°$ in Figure 1). The dashed line in Figure 1 represents the energy barrier to interconversion of the respective

(10) Adams, C. S.; Legzdins, P.; McNeil, W. S. *Organometallics* **2001**, *20*, 4939−4955.

(11) For details on how the interpretations of the chemistry vary with the nature of the reactive species, see ref 10 and the illustrations therein.

(12) For the three other reported examples of intermolecular C−H activations by alkylidene complexes, see: (a) Coles, M. P.; Gibson, V. C.; Clegg, W.; Elsegood, M. R. J.; Porrelli, P. A. *J. Chem. Soc., Chem. Commun.* **1996**, 1963−1964. (b) van der Heijden, H.; Hessen, B. *J. Chem. Soc., Chem. Commun.* **1995**, 145−146. (c) Cheon, J.; Rogers, D. M.; Girolami, G. S. *J. Am. Chem. Soc.* **1997**, *119*, 6804−6813.

(13) Note that the ortho aryl product is also observed as a trace product (~1% overall) in the activation of toluene by σ-**A**.

Scheme 2

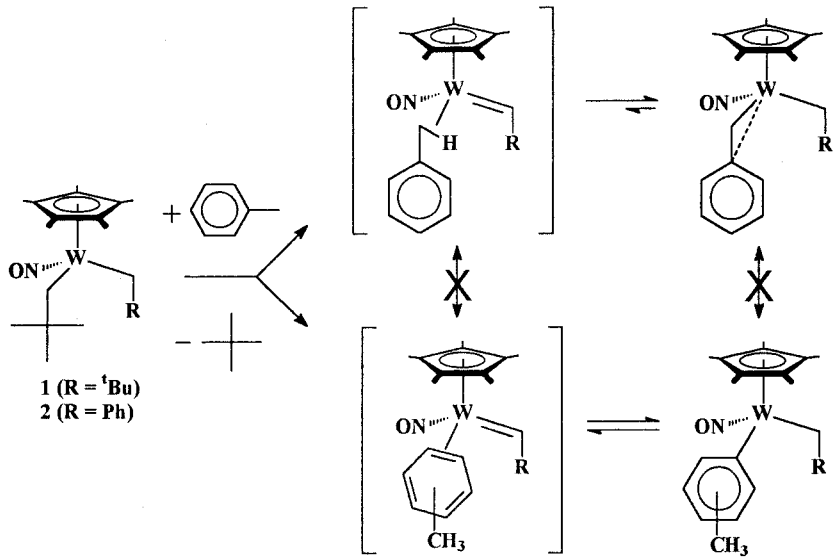

π-arene and σ-phenylmethane complexes, which in these systems is higher than the barriers to C−H bond scission.

As part of our continuing effort to understand the activation chemistry exhibited by these alkylidene systems, we have conducted an investigation into the activation of other substituted arenes, namely, the xylenes, mesitylene, and α,α,α-trifluorotoluene, by **1** and **2**. The principal objectives of this effort were to determine how the properties of the arene substrate influence the aryl vs benzyl and aryl regioisomer product distributions and to establish the factors controlling these distributions. The results of this investigation are presented herein.

Results and Discussion

Thermolysis of 2 in Xylenes. Complex **2** has been thermolyzed in *m*-, *o*-, and *p*-xylene for 40 h at 70 °C. Thermolysis of **2** in *m*-xylene under these conditions results in the formation of two products, namely, Cp*W(NO)($CH_2C_6H_5$)(C_6H_3-3,5-Me_2) (**3**) and Cp*W(NO)($CH_2C_6H_5$)($CH_2C_6H_4$-3-Me) (**4**), in >95% overall yield as determined by ^{1}H NMR spectroscopy (eq 1).[14] The product ratios obtained from two independent experi-

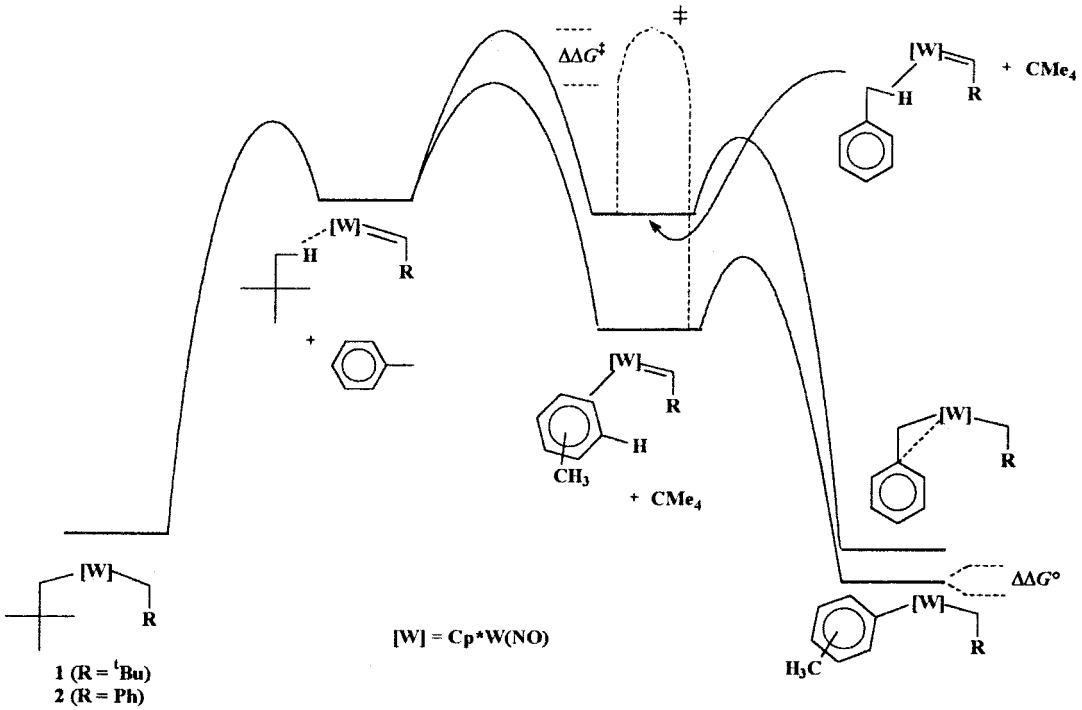

Figure 1. Qualitative free energy vs reaction coordinate diagram for the activation of toluene by σ-**A** and σ-**B**.

ments are the same within experimental error (9.1 ± 0.5:1 and 9.4 ± 0.5:1 (95% CI)). No signals attributable to any additional C−H activation products are evident in the ^{1}H NMR spectrum of the final reaction mixture.

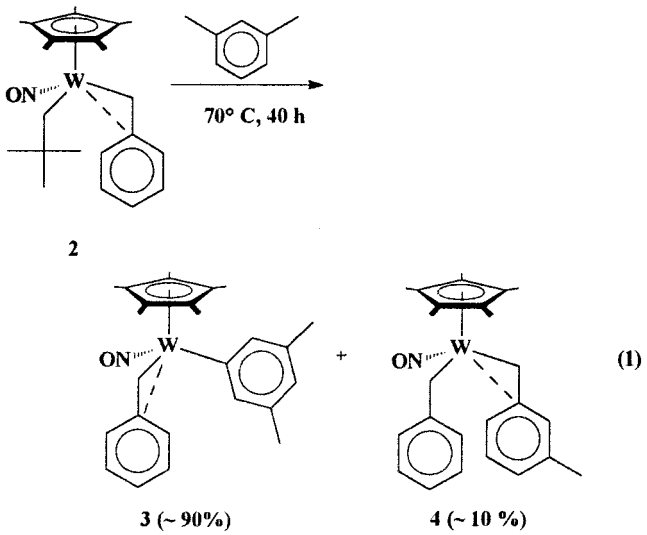

The major product, **3**, has been isolated by crystallization from Et_2O/hexanes (3:1) in sufficient yield (29%) to permit its full characterization. Most notably, the ^{1}H NMR spectrum of **3** in CD_2Cl_2 exhibits a broad, upfield signal for the ortho H atoms (6.29 ppm, 21 Hz at half-height). Similar spectral features are observed for ortho H protons in other hydrocarbyl complexes containing methylaryl ligands (vide infra).[15] The low chemical shift for the ipso carbon resonance (114.8 ppm) in its ^{13}C{^{1}H}NMR spectrum is indicative of an η^2-benzyl ligand, on average, in solution. This structural feature is common in the ground-state conformations of these types of benzyl complexes both in solution and in the solid state (vide infra).[16−18]

The minor product, **4**, has been identified by spectroscopic analysis of the final reaction mixture. It has also been prepared independently via the metathesis reaction of Cp*W(NO)($CH_2C_6H_5$)Cl and (3-Me-$C_6H_4CH_2$)$_2$Mg·*x*(dioxane) in THF to confirm its identity. The most notable spectral features of **4** are the two distinct ipso carbon resonances in its ^{13}C{^{1}H}NMR spectrum (113.9 and 142.3 ppm) and the correlation of the pair of methylene resonances that have the lower chemical shifts with the benzyl ligand rather than the 3-methylbenzyl ligand. These spectroscopic features indicate that the more sterically demanding 3-methylbenzyl ligand is attached in an η^2 fashion to the tungsten center on average in solution, while the benzyl ligand is η^1.[16,17]

Similar results are obtained from the thermolysis of **2** in *o*- and *p*-xylene. In *o*-xylene, the two products of solvent C−H activation, namely, Cp*W(NO)($CH_2C_6H_5$)(C_6H_3-3,4-Me_2) (**5**) and Cp*W(NO)($CH_2C_6H_5$)($CH_2C_6H_4$-2-Me) (**6**), form in a 14.6 ± 0.4:1 ratio (eq 2). In *p*-xylene, the products, Cp*W(NO)($CH_2C_6H_5$)(C_6H_3-2,5-Me_2) (**7**) and Cp*W(NO)($CH_2C_6H_5$)($CH_2C_6H_4$-4-Me) (**8**), are produced in a 6.2 ± 0.4:1 ratio (eq 3).

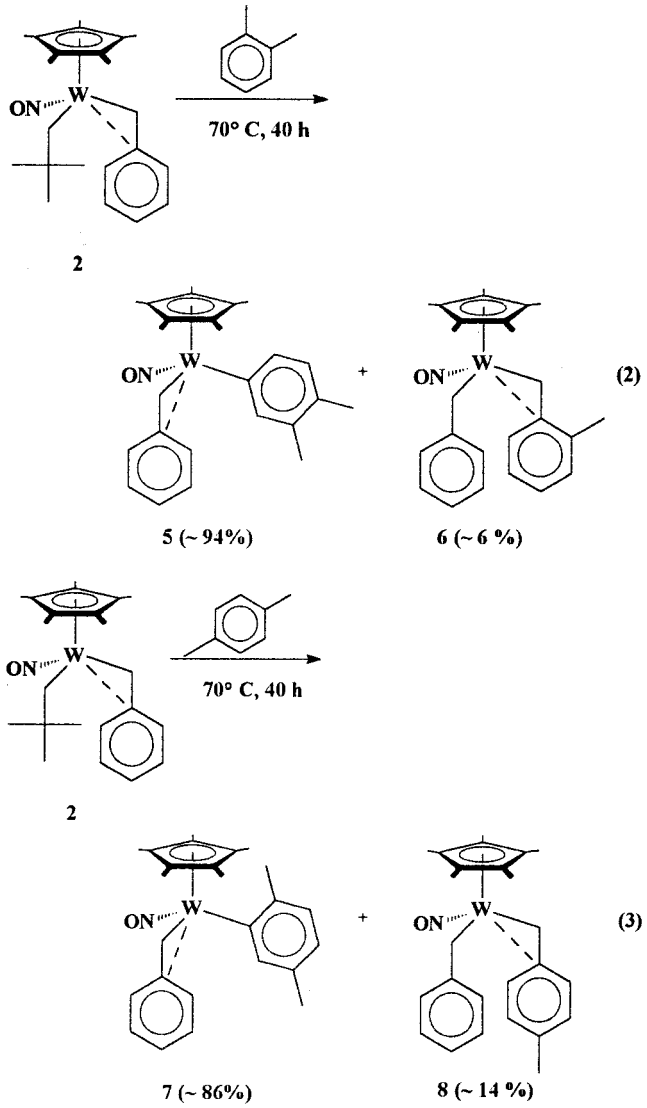

The major aryl products, **5** and **7**, have been isolated by crystallization from Et_2O/hexanes in adequate yield (30−40%) to permit full characterization. Both **5** and **7** have features similar to **3**, namely, signals due to η^2-benzyl ligands and broadened, downfield resonances for the ortho H atoms of the aryl ligands. Complex **7** also exhibits broadened signals for one of the methyl groups of the 2,5-dimethylaryl ligand and the synclinal methylene H atom of the benzyl ligand (vide infra).

Solid-State Molecular Structure of Complex 7. The solid-state molecular structure of **7** has been established by a single-crystal X-ray crystallographic analysis. The resulting ORTEP diagram is shown in Figure 2, and pertinent crystal data and solution and refinement data are collected in Tables 1 and 2, respectively. The three-legged piano-stool structure clearly has a η^2-benzyl ligand, which is characterized by a short W−C_{ipso} bond distance (W(1)−C(2) = 2.554(4) Å) and the acute W−C−C_{ipso} bond angle (W(1)−C(1)−C(2) =

(14) A small amount of decomposition (<5%) is also observed. The signals for the decomposition products increase upon prolonged reaction times and are also observed when pure complex **3** is thermolyzed independently (vide infra). Several related aryl products have been shown to be moderately thermally unstable in other instances (vide infra).

(15) Debad, J. D.; Legzdins, P.; Batchelor, R. J.; Einstein, F. W. B. *Organometallics* **1993**, *12*, 2094−2102.

(16) Dryden, N. H.; Legzdins; Trotter, J.; Yee, V. C. *Organometallics* **1991**, *10*, 2857−2870.

(17) Legzdins, P.; Jones, R. H.; Phillips, E. C.; Yee, V. C.; Trotter, J.; Einstein, F. W. B. *Organometallics* **1991**, *10*, 986−1002.

(18) Bau, R. Mason, S. A.; Patrick, B. O.; Adams, C. S.; Sharp, W. B.; Legzdins, P. *Organometallics* **2001**, *20*, 4492−4501.

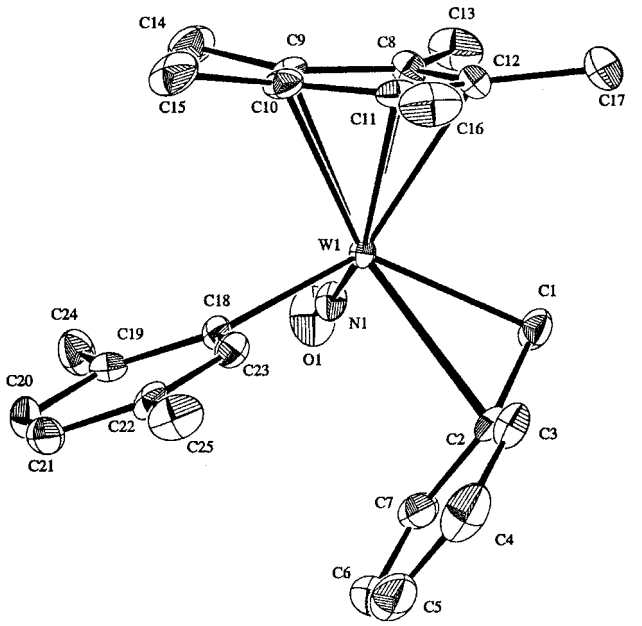

Figure 2. ORTEP plot of the solid-state molecular structure of Cp*W(NO)($CH_2C_6H_5$)(C_6H_3-2,5-Me_2) (**7**) with 50% probability ellipsoids. Selected bond lengths (Å) and angles (deg): W(1)−C(1) = 2.191(4), W(1)−C(2) = 2.554(4), W(1)−C(18) = 2.181(3), N(1)−O(1) = 1.224(4), W(1)−N(1)−O(1) = 169.3(3), W(1)−C(1)−C(2) = 86.4(3), C(18)−W(1)−C(2) = 124.7(1), N(1)−W(1)−C(18) = 98.6(1), W(1)−C(18)−C(19) = 128.2(2), W(1)−C(18)−C(23) = 115.5(3), N(1)−W(1)−C(18)−C(19) = − 23.3(4), W(1)−C(18)−C(23)−C(22) = −179.0(3).

Table 1. Crystal Data for Complexes 7 and 9

	7	**9**
empirical formula	$C_{25}H_{31}NOW$	$C_{26}H_{33}NOW$
cryst habit, color	red-brown block	orange, chip
cryst size (mm)	0.50 × 0.44 × 0.20	0.50 × 0.40 × 0.20
cryst syst	triclinic	monoclinic
space group	$P\bar{1}$ (#2)	$P2_1/a$ (#14)
volume (Å^3)	1071.6(2)	2271.2(2)
a (Å)	8.5023(9)	8.7551(5)
b (Å)	8.6298(9)	27.187(1)
c (Å)	15.805(1)	9.7641(5)
α (deg)	74.510(2)	90
β (deg)	79.936(2)	102.254(4)
γ (deg)	74.797(3)	90
Z	2	4
density(calcd) (Mg/m^3)	1.690	1.630
abs coeff (cm^{-1})	54.11	51.08
F_{000}	540	1104

86.4(3)°). Another interesting feature of the structure involves the metrical parameters of the 2,5-dimethylphenyl ligand and its preferred orientation. The W(1)−C(18)−C(19) bond angle to the ortho carbon (128.2(2)°) is distorted from the expected angle of 120°. This conformation places the ortho methyl group cis to the NO ligand (N(1)−W(1)−C(18)−C(19) = − 23.3(4)°), even though the trans orientation has the largest gap between the three legs of the piano-stool molecule (C(18)−W(1)−C(2) = 124.7(1)° vs N(1)−W(1)−C(18) = 98.6(1)°). Similar *cis*-NO conformations and M−C bond distortions (M−C−C_{ortho} = ∼130 °) have also been found for the *o*-methyl aryl ligands in the solid-state molecular structures of the complexes CpW(NO)(C_6H_4-2-Me)(C_6H_4-3-Me),[19] Cp*W(NO)(CH_2CMe_3)(C_6H_4-2-Me),[15] Cp*W(NO)-(C_6H_4-2-$Me)_2$, and Cp*Mo(NO)(C_6H_4-2-$Me)_2$.[20] Interestingly, the general class of aryl complexes (i.e., Cp′M(NO)(R)(R′) (Cp′ = Cp, Cp*; M = Mo, W; R = aryl; R′ = aryl, benzyl, alkyl) are generally thermally sensitive (vide supra),[9,19,20] and the dominant mode of decomposition appears to involve *β*-H elimination.[19,21] The *β*-H elimination proclivities of these aryl complexes may be due to the strained *cis*-NO orientation of the aryl ligands and the corresponding close proximity of the *β*-H linkage of the aryl ligand to the metal-centered LUMO.

Thermolysis of 2 in Mesitylene. This thermolysis (70 °C, 40 h) results in the formation of only one C−H activation product, namely, Cp*W(NO)($CH_2C_6H_5$)-($CH_2C_6H_3$-3,5-Me_2) (**9**) in >95% yield (eq 4).

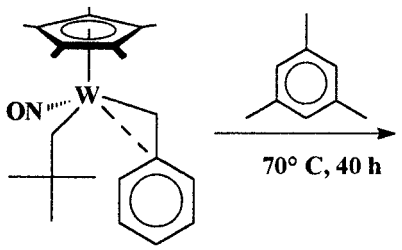

2

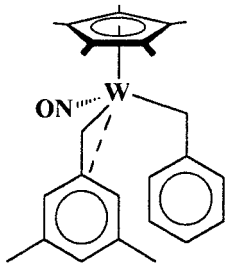

9 **(4)**

Complex **9** exhibits spectral features typical of the mixed benzyl complexes reported above. In particular, its ^{1}H and ^{13}C{^{1}H} NMR data indicate that it is the bulky mesityl ligand and not the benzyl ligand that is attached to the metal in an η^2 fashion on average in solution. This conclusion is supported by the solid-state molecular structure of **9**. The ORTEP plot of the structure (Figure 3) clearly shows an η^2-mesityl ligand with a bonding contact between the ipso carbon and the metal center (W(1)−C(2) = 2.391(4) Å) and an acute W−C−C_{ipso} bond angle (83.7(2)°). From these data, as well as from the data for **4**, it appears that in mixed benzyl complexes of the type Cp*W(NO)(CH_2Ar)-(CH_2Ar-Me_x) the methyl-substituted benzyl ligand is preferentially attached in an η^2 fashion despite the resulting increase in steric congestion at the metal center. Presumably, the controlling factor in these situations is the increased electron-donor capability of the more electron-rich substituted phenyl ring.

Thermolysis of 1 in *p*-Xylene. At the outset of these investigations, it was our expectation that the products resulting from the activation of substituted arenes by **1** would include complexes of the type produced by **2** under similar conditions (vide supra). Indeed, the ther-

(19) Sharp, W. B. Ph.D. Dissertation, University of British Columbia, 2001.

(20) Dryden, N. H.; Legzdins, P.; Rettig, S. J.; Veltheer, J. E. *Organometallics* **1992**, *11*, 2583−2590.

(21) Debad, J. D. Ph.D. Dissertation, University of British Columbia, 1994.

Table 2. Data Refinement and Structural Solution and Refinement Data for Complexes 7 and 9

	7	9
	Data Collection and Refinement	
data images	464 exposures at 12.0 s	464 exposures at 15.0 s
ϕ oscillation range ($\chi = 0$) (deg)	0.0−190.0	0.0−190.0
ω oscillation range ($\chi = 90$) (deg)	−19.0−23. 0	−19.0−23. 0
detector swing angle (deg)	−5.50	−5.56
$2\theta_{max}$ (deg)	55.8	55.8
detector position (mm)	40.69	40.58
measured reflns: total	8915	14628
Unique	4030 ($R_{int} = 0.031$)	4763 ($R_{int} = 0.043$)
	Structure Solution and Refinement	
structure solution method	Patterson	Direct
refinement	full-matrix least-squares	full-matrix least-squares
no. observations	4030	4653
no. variables	253	262
final R indices[a]	R1 = 0.026, wR2 = 0.036	R1 = 0.027, wR2 =0.049
no. observations ($I > 3\sigma(I)$)	3801	3870
goodness-of-fit on F^2[b]	1.31	1.06
largest diff peak and hole (e Å^{-3})	1.73 and −2.53	0.98 and − 1.43

[a] R1 on $F = \Sigma(|F_o| - |F_c|)\ |/\Sigma|F_o|$; wR2 = $[\Sigma(w(|F_o|^2 - |F_c|^2)^2)/\Sigma wF_o^4]^{1/2}$; $w = [\ \sigma^2F_o^2]^{-1}$. [b] GOF = $[\Sigma(w(|F_o| - |F_c|)^2)/(\text{degrees of freedom})]^{1/2}$.

molysis of **1** in *p*-xylene for 40 h at 70 °C generates products from the activation of one and two molecules of xylene (eq 5). The two products derived from the activation of one solvent molecule are Cp*W(NO)-(CH_2CMe_3)(C_6H_3-2,5-Me_2) (**10**) and the previously characterized Cp*W(NO)(CH_2CMe_3)($CH_2C_6H_4$-4-Me) (**11**).[16] The other two complexes derived from the activation of two solvent molecules are Cp*W(NO)($CH_2C_6H_4$-4-Me)(C_6H_4-2,5-Me_2) (**12**) and the previously characterized Cp*W(NO)($CH_2C_6H_4$-4-$Me)_2$ (**13**).[16] The ratio of the four products is **10**:**11**:**12**:**13** = 1.81 ± 0.09:0.44 ± 0.05:1.0:0.15 ± 0.02.

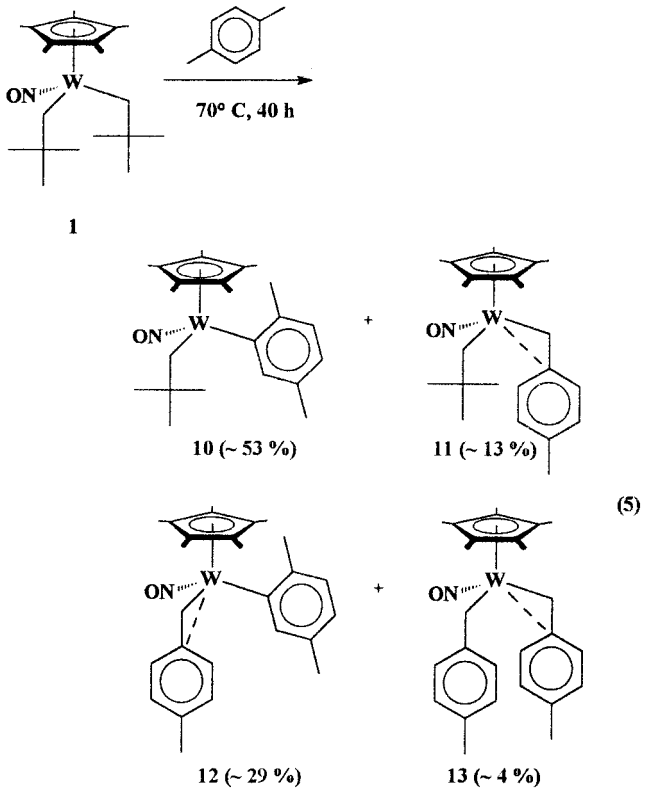

(5)

Complexes **10** and **12** have been isolated in pure form from the final reaction mixture by chromatography on alumina I. The NMR spectra of **12**, like those of the related complex **7**, reveal the presence of an η^2 4-methylbenzyl ligand and exhibit broad resonances for the ortho H atom, one methyl group of the 2,5-dimethylphenyl ligand, and the synclinal methylene H atom of the benzyl ligand. The NMR spectral features of **10** are also noteworthy since only signals attributable to the Cp* and *tert*-butyl ligands, one of the methyl groups, and two aryl H atoms are present in its room-temperature ^{1}H NMR spectrum. NMR analysis of the toluene-d_8 solution of **10** at lower temperatures (≤10 °C) reveals that these features are probably due to two rapidly interchanging isomers. In the EXSY spectra recorded at 213 K, exchange is observed between the methylene, aromatic, and methyl signals of the two isomers, thereby indicating that the interchange involves rotation of one

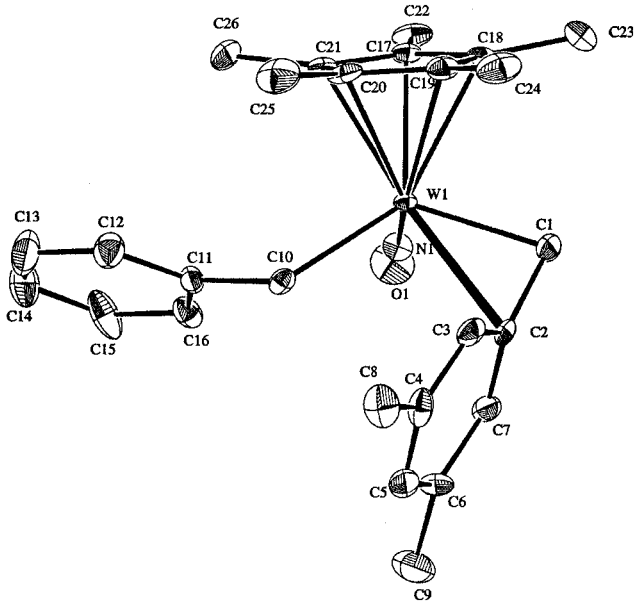

Figure 3. ORTEP plot of the solid-state molecular structure of Cp*W(NO)($CH_2C_6H_5$)($CH_2C_6H_3$-3,5-Me_2) (**9**) with 50% probability ellipsoids. Selected bond lengths (Å) and angles (deg): W(1)−C(1) = 2.181(4), W(1)−C(2) = 2.391(4), W(1)−C(10) = 2.225(4), N(1)−O(1) = 1.231(4), C(1)−C(2) = 1.467(6), C(10)−C(11) = 1.500(5), W(1)−N(1)−O(1) = 170.4(3), W(1)−C(10)−C(11) = 83.7(2), W(1)−C(10)−C(11) = 120.1(3).

or both of the neopentyl and 2,5-dimethylphenyl ligands about their W−C linkages. Presumably, the broad NMR spectral features exhibited by **7**, **12**, and the other aryl products reported here are manifestations of similar rotational phenomena.

Thermolysis of 1 in Mesitylene. This thermolysis for 40 h at 70 °C results in formation of two C−H activation products, namely, the product of benzylic sp^3 C−H bond activation of one solvent molecule, Cp*W(NO)(CH_2CMe_3)($CH_2C_6H_3$-3,5-Me_2) (**14**), and the product of similar activations of two solvent molecules, Cp*W(NO)($CH_2C_6H_3$-3,5-Me_2)$_2$ (**15**). The products are present in the final reaction mixture in a 1:3.6 ± 0.4 ratio (eq 6). Complex **15** has been isolated in crystalline form from the reaction mixture and has been fully characterized, while complex **14** is readily identifiable by its spectroscopic features in the ^{1}H NMR spectrum of the final reaction mixture. There is no evidence for the formation of either of the related aryl products of aromatic sp^2 C−H bond activation in the ^{1}H NMR spectrum.

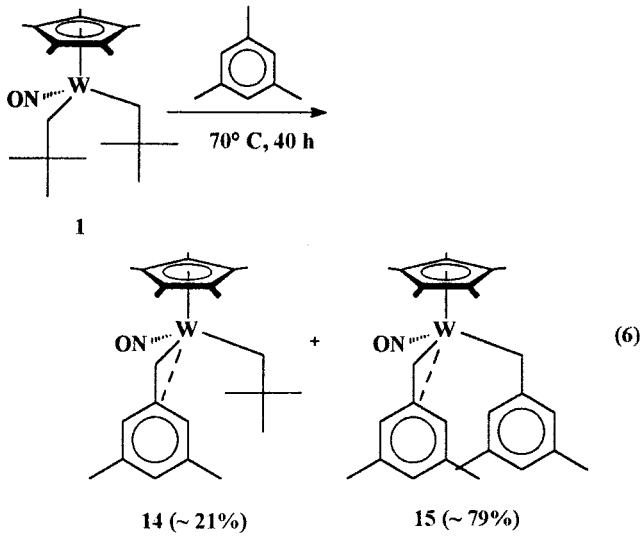

(6)

The thermolysis of **1** in mesitylene has also been conducted for 15 and 64 h at 70 °C. In the 15 h ^{1}H NMR spectrum, the ratio of **14**:**15** is ~2:1, while in the 64 h spectrum only signals due to **15** are observed. These shifts in product distributions over time are fully consistent with the formation of **15** via the decomposition of **14** to its benzylidene derivative. It thus appears that complexes of the type Cp*W(NO)(CH_2CMe_3)(CH_2Ar-Me_x) decompose thermally to their respective C−H activating benzylidene complexes, Cp*W(NO)(=CHAr-Me_x). Interestingly, the ratio of aryl vs benzyl products of *p*-xylene activation derived from **11** (**12**:**13** = 6.6 ± 0.9:1) is the same as that derived from **2** within experimental error (**7**:**8** = 6.2 ± 0.4:1). Hence, the presence of a para methyl group on the phenyl ring of the reactive benzylidene intermediate does not appear to influence the outcome of the C−H activation chemistry.

Activation of α,α,α-Trifluorotoluene. Thermolysis of **2** in α,α,α-trifluorotoluene cleanly generates two aryl products, namely, the meta and para isomers Cp*W(NO)($CH_2C_6H_5$)(C_6H_4-3-CF_3) (**16a**) and Cp*W(NO)($CH_2C_6H_5$)(C_6H_4-4-CF_3) (**16b**) in a 2.27 ± 0.03:1 ratio (eq 7). The isomers can be isolated as a crystalline mixture (39% yield, vide infra) and are readily differentiated by distinctive patterns in the aromatic region of the ^{1}H NMR spectrum. The other spectral features of **16a**,**b** are consistent with those exhibited by the other benzyl aryl complexes reported above. No evidence was obtained for the formation of the ortho isomer or products from C−F activation. ^{1}H NMR spectroscopic analysis of the reaction mixture obtained from the partial thermolysis of **2** after only 15 h of heating in α,α,α-trifluorotoluene at 70 °C reveals that the product ratios are invariant with time.

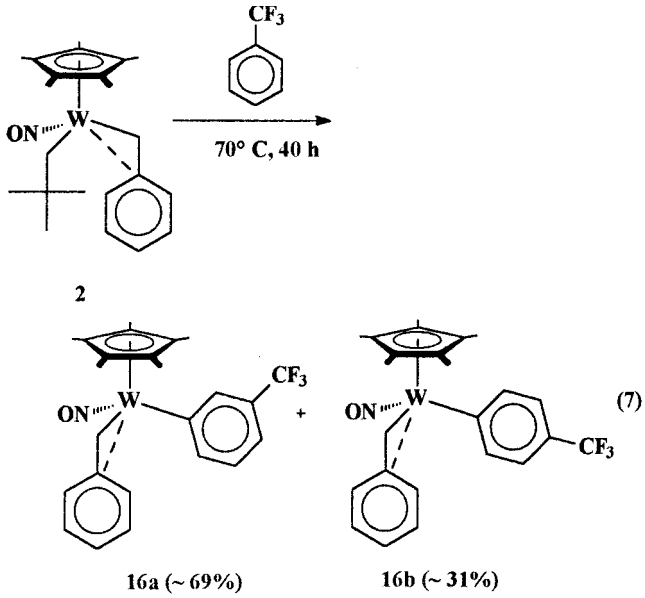

(7)

Thermolysis of **1** in α,α,α-trifluorotoluene also generates the meta and para aryl products of C−H activation, namely, Cp*W(NO)(CH_2CMe_3)(C_6H_4-3-CF_3) (**17a**) and Cp*W(NO)(CH_2CMe_3)(C_6H_4-4-CF_3) (**17b**) in a 1.85 ± 0.06:1 ratio (eq 8). The isomers can also be isolated as a crystalline mixture (38% yield, vide infra), and the spectral properties of **17a**,**b** are typical of the other aryl products reported above. ^{1}H NMR spectroscopic monitoring of the reaction mixture again reveals that the product ratio is invariant with time.

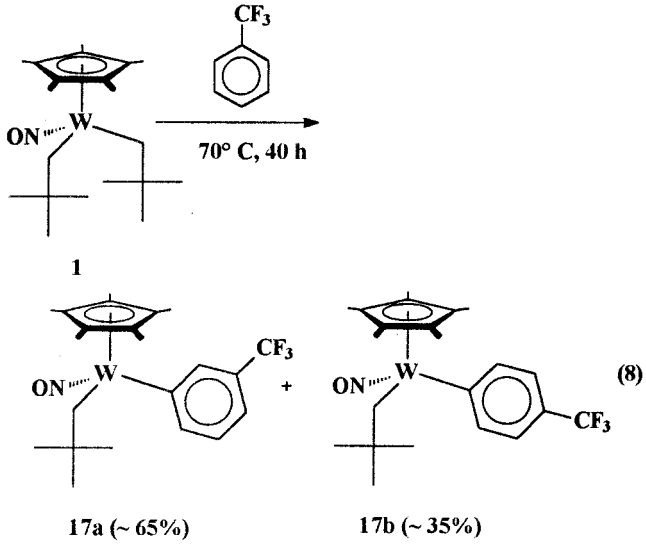

(8)

Trends in the Product Distributions Derived From the C−H Activation of Substituted Arenes.

Table 3. Relative Aryl vs Benzyl Product Distributions Obtained from the Thermolysis of 1 and 2 in Methyl-Substituted Arene Solvents

reagent	solvent	relative product ratio (aryl:benzyl)
2	toluene	18.6 ± 1.2:1
2	*o*-xylene	14.6 ± 0.4:1
2	*m*-xylene	9.3 ± 0.7:1[a]
2	*p*-xylene	6.2 ± 0.4:1
2	mesitylene	0:100
1	toluene	4.2 ± 0.3:1[b]
1	*p*-xylene	1.14 ± 0.7:1[c]
1	mesitylene	0:100

[a] Average and uncertainty (95% CI) from two independent experiments. [b]Ratio from integrals for neopentyl aryl products vs benzyl activation products. See ref 9 for details. [c]Ratio from integrals for **10**: (**11** + **12** + **13**).

Table 4. Relative Distributions of Meta and Para Aryl Regioisomers from the Thermolyses of 1 and 2 in Toluene and α,α,α-Trifluorotoluene

reagent	solvent	relative product ratio (meta:para)
2	toluene	1.97 ± 0.11:1
1	toluene	1.45 ± 0.08:1[a]
2	α,α,α-trifluorotoluene	2.27 ± 0.03:1
1	α,α,α-trifluorotoluene	1.85 ± 0.06:1

[a] The ortho tolyl isomer is also present in ∼1% abundance relative to the meta and para isomers combined. See ref 9 for details.

The relative product distributions resulting from the thermolysis of **1** and **2** in the selected arene solvents described above are collected together in two tables, one summarizing the distributions of aryl vs benzyl C−H activation products (Table 3), the other summarizing the distributions of aryl regioisomers (Table 4). These tables also include the previously reported data for the activation of toluene for comparison purposes.

Tables 3 and 4 reveal several interesting features. For example, in the aryl vs benzyl product distributions derived from the activation of toluene, xylene, and mesitylene by *σ*-**A** and *σ*-**B**, the benzyl products are increasingly favored as the number of methyl substituents increases. Likewise, the movement of the methyl groups from the ortho to meta to para position in the xylenes shifts the aryl vs benzyl product distribution toward the benzyl products (aryl:benzyl for *o*-xylene > *m*-xylene > *p*-xylene). With respect to the aryl product regioselectivities, only the least sterically congested aryl regioisomers are formed in the activations of *o*-xylene and *m*-xylene, while the meta and para aryl products are formed preferentially over ortho aryl products for both α,α,α-trifluorotoluene and toluene, despite the change in the substituent from CH_3 to CF_3. However, in the latter case, there is a slight shift toward the meta isomer upon replacement of CH_3 with the CF_3 group for the activations mediated by both *σ*-**A** and *σ*-**B**. Finally, the distributions obtained from *σ*-**B** are more abundant in the aryl products than those obtained from *σ*-**A** in both mono- and disubstituted solvents (toluene, *p*-xylene). Likewise, the aryl regioisomer distributions obtained from the activations of α,α,α-trifluorotoluene and toluene by *σ*-**B** favor the meta isomer over the para and ortho isomers, more so than the distributions obtained from *σ*-**A**.

Rationales of the Observed Trends. There appear to be several common features and trends in the product selectivities derived from the activation of substituted arenes as outlined above. However, it remains to be determined if these selectivities are governed by the same factors as those previously identified for toluene.[9,10] Each of the arene systems is thus considered separately in the discussion that follows.

Xylenes. In the case of the xylenes, only one aryl regioisomer is formed in each instance. Hence, only the origin of the aryl vs benzyl product selectivities needs to be determined. To that end, four selected products of xylene C−H activation have been thermolyzed at 70 °C in the parent solvent (i.e., *m*-, *o*-, or *p*-xylene) and in benzene-d_6. The first product, the benzyl complex derived from sp^3 C−H bond activation of *m*-xylene by *σ*-**B**, namely, Cp*W(NO)($CH_2C_6H_5$)($CH_2C_6H_4$-3-Me) (**4**), is thermally robust, exhibiting no chemical transformations after 40 h of heating in either solvent. Thus, the formation of **4** is effectively irreversible under the thermolysis conditions. In contrast, the aryl product of sp^2 C−H bond activation of *p*-xylene, namely, Cp*W(NO)($CH_2C_6H_5$)(C_6H_3-2,5-Me_2) (**7**), *does* interconvert to the corresponding benzyl product of sp^3 C−H bond activation, Cp*W(NO)($CH_2C_6H_5$)($CH_2C_6H_4$-4-Me) (**8**), when heated in *p*-xylene, albeit rather slowly. A ∼95:5 ratio of **7**:**8** can be detected by ^{1}H NMR spectroscopy of the reaction mixture obtained after heating **7** in *p*-xylene for 40 h at 70 °C. Some decomposition (∼10%) also occurs. Since the distribution of **7**:**8** at 40 h is ∼86:14 when derived from **2**, the isomerization does not appear to be fast enough to attain equilibrium under these conditions. When the thermolysis of **7** is conducted in benzene-d_6, only a trace amount (<1%) of the product of benzene-d_6 activation, namely, the previously characterized Cp*W(NO)($CHDC_6H_5$)(C_6D_5),[9] is observed over the same time period. Consequently, the majority of the isomerization of **7** to **8** appears to occur via an *intra*molecular process rather than by dissociation of *p*-xylene. The mostly likely intramolecular process is the interconversion of the respective *π*-arene and *σ*-arylmethane complexes, the former being formed by reversible sp^2 C−H bond scission (Scheme 3). For consistency, the term "*σ*-arylmethane complex" is used throughout as a generic term for the (sp^3-C,H) bound *σ*-complex of substituted arenes.

The thermolyses of two other aryl products, the benzyl *m*-xylyl complex Cp*W(NO)($CH_2C_6H_5$)(C_6H_3-3,5-Me_2) (**3**) and the neopentyl 2,5-dimethylphenyl complex Cp*W(NO)(CH_2CMe_3)(C_6H_3-2,5-Me_2) (**10**), in the respective parent solvents and benzene-d_6, also reveal trace amounts (<2%) of conversion to the corresponding benzyl products of sp^3 C−H bond activation, namely, Cp*W(NO)($CH_2C_6H_5$)($CH_2C_6H_4$-3-Me) (**4**) and Cp*W(NO)(CH_2CMe_3)($CH_2C_6H_4$-4-Me) (**11**). It thus appears that, unlike those derived from toluene, the aryl products derived from the xylenes can intramolecularly isomerize to the corresponding benzyl products. However, since the conversion of aryl to benzyl products is quite slow on the thermolysis time scale, the aryl vs benzyl product distributions observed for the activation of xylenes are mostly kinetic in origin. Hence, just as for toluene, the magnitudes of the aryl vs benzyl product selectivities listed in Table 3 chiefly arise from the relative rates of coordination of the xylene substrate in the *π*-arene and *σ*-arylmethane fashions ($\Delta\Delta G^{\ddagger}$ in

Scheme 3

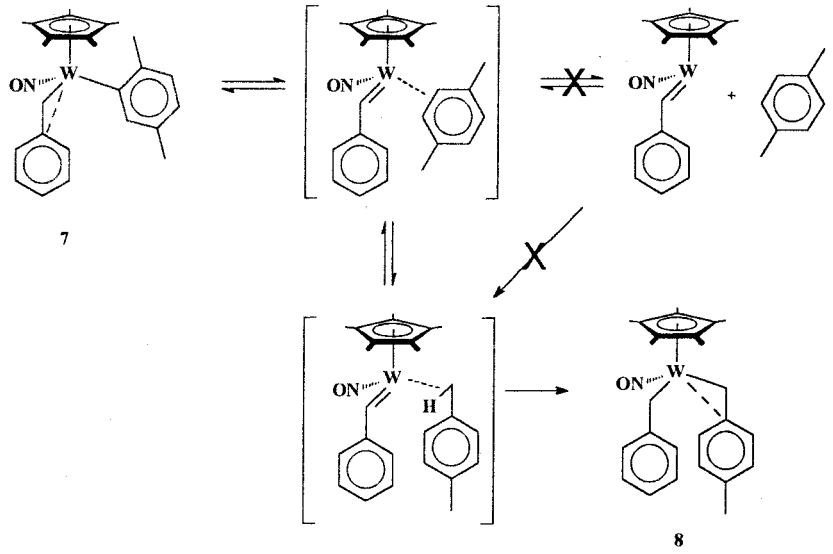

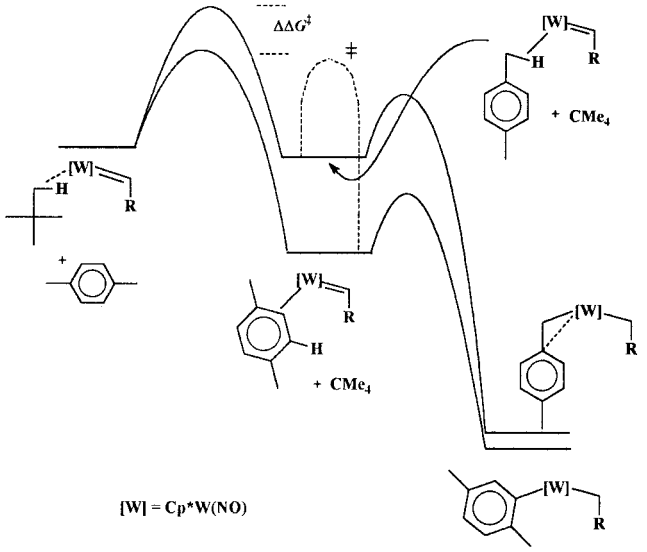

Figure 4. Qualitative representation of the free energy vs reaction coordinate diagram for the activation of xylenes by *σ*-**A** and *σ*-**B**, using *p*-xylene as an illustrative example.

Figure 4). According to this interpretation, the shifts from aryl products toward the benzyl products upon moving from *p*- to *m*- to *o*-xylene activation by *σ*-**B** therefore arise from reductions in the relative energy barriers to formation of the respective *π*-arene and *σ*-arylmethane complexes. Presumably, this is due to increased steric interactions in the *π*-arene complexes as more of the *π*-ring is shielded by the methyl substituents. The aryl-to-benzyl product isomerizations of **7** to **8**, **3** to **4**, and **10** to **11** can likewise be explained by an energy barrier for interconversion of the *π*-arene complex to the *σ*-arylmethane complex (i.e., the dashed line in Figure 4) that is lower than the corresponding barrier in the reaction coordinate for toluene activation (Figure 1). The isomerization may also be statistically assisted by the increased number of methyl C−H bonds and corresponding *σ*-arylmethane complexes as compared to the number of possible *π*-arene complexes for toluene and the xylenes. On the other hand, the fact that the reverse process, namely, isomerization of **4** to **3**, is not observed is likely due to the higher energy barrier for reversion to the *σ*-arylmethane complex, as well as the existence of an additional η^2-benzyl conformation in the benzyl activation products which have to convert to the less stable η^1 form to undergo reversible C−H bond scission. Finally, according to this interpretation, the fact that *p*-xylene activation by *σ*-**B** leads to a higher relative amount of the aryl product than *σ*-**A** (6.2 ± 0.4:1 vs 1.14 ± 0.07:1) is due to a greater difference in the relative transition state energies for *π*-arene vs *σ*-arylmethane coordination. This phenomenon may well arise from diminished steric interactions between the xylene substrate and the benzylidene ligand of *σ*-**B**, as compared to the bulkier neopentylidene ligand of *σ*-**A**, in the formation of the more sterically congested *π*-arene complexes.

Mesitylene. Mesitylene is the only case in which the formation of the benzyl product of C−H activation is favored over the corresponding aryl product. Given that the activation process for this substrate should be similar to that of toluene and the xylenes, three factors may be responsible for the inversion in product selectivity. One factor is that the transition-state energies for formation of the *π*-arene complexes leading to sp^2 C−H bond scission may be higher, rather than lower, in energy than those for formation of the *σ*-arylmethane complexes leading to the benzyl product, due to the presence of unfavorable steric interactions in the former type of complex. Alternatively, the barrier for isomerization of the *π*-arene complex to the *σ*-arylmethane complex may be lower than for scission of the sp^2 C−H bond so that only the *σ*-arylmethane complex leads to substrate C−H bond scission. Finally, the statistical dominance of sp^3 C−H bonds compared to sp^2 C−H bonds means that, unlike toluene and the xylenes, there is a prevalence of *σ*-arylmethane complexes vs *π*-arene complexes. Either one or any combination of these factors could lead to the preferential formation of the benzyl product of sp^3 C−H bond activation.

α,α,α-Trifluorotoluene. The activation of α,α,α-trifluorotoluene by *σ*-**A** yields the meta and para aryl C−H activation products in a ratio (1.85 ± 0.06:1) that does not change during the course of the thermolysis of **1** in this solvent. Fortuitously, whether this distribution

Scheme 4

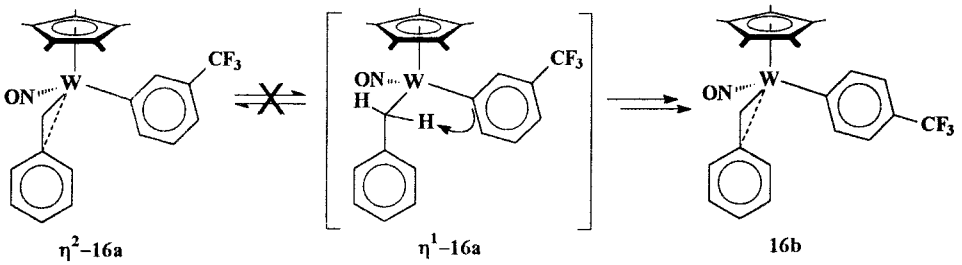

is under kinetic or thermodynamic control can be determined since **17a** and **17b** cocrystallize in a mixture that significantly favors **17a** over **17b** (~11.5:1). Monitoring the thermolysis of this mixture in benzene-d_6 by ^{19}F NMR spectroscopy over 6 h reveals that **17a** isomerizes to the thermodynamic mixture of **17a**,**b** (eq 9). Presumably, the mechanism for this isomerization involves reversible sp^2 C−H bond cleavage. A nonlinear least-squares analysis of the data from the reaction using an exponential approach to equilibrium kinetic model yields a calculated k_{obs} of $1.2 \pm 0.01 \times 10^{-4}$ s^{-1} (see Supporting Information for details). After statistical correction this corresponds to rate constants of 4.1×10^{-5} s^{-1} for the isomerization of **17a** to **17b** and 3.9×10^{-5} s^{-1} for the opposite reaction. The calculated K_{eq} is 0.53 ± 0.01, which agrees with the experimental value of 0.54. The equilibration of **17a**,**b** under thermolysis conditions implies that the distribution of complexes **17a**,**b** derived from the thermolysis of **1** in this solvent is under thermodynamic control. Thus, as in the case of toluene, the product distribution listed in Table 4 appears to arise from the relative energies of the meta and para isomers themselves.

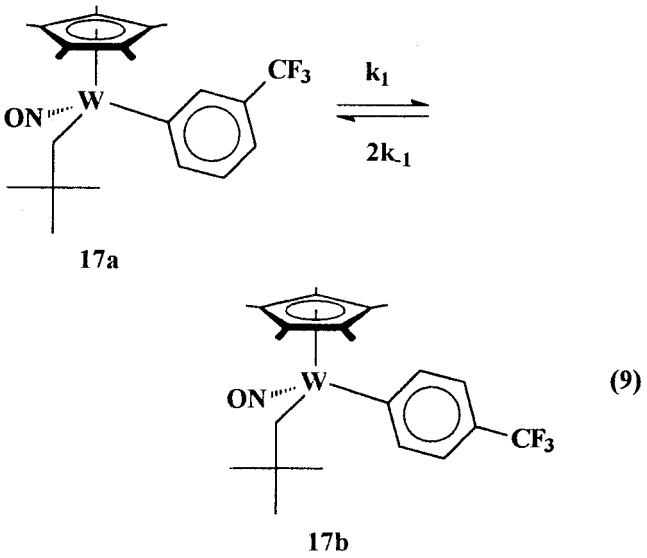

(9)

The activation of α,α,α-trifluorotoluene by *σ*-**B** generates the meta and para aryl products Cp*W(NO)(CH$_2$C$_6$H$_5$)(C$_6$H$_4$-3-CF$_3$) (**16a**) and Cp*W(NO)(CH$_2$C$_6$H$_5$)(C$_6$H$_4$-4-CF$_3$) (**16b**) in a 2.27 ± 0.03:1 ratio. This ratio also remains constant over the course of the reaction. In addition, as with **17a**,**b**, complexes **16a**,**b** cocrystallize in a mixture enriched in **16a** (8.3:1), thereby permitting an analysis of the nature of the distribution of **16a**,**b**. Interestingly, the thermolysis of this mixture in benzene-d_6 reveals that **16a** *does not isomerize at all* to **16b** even after 40 h at 70 °C (eq 10). Hence, in this particular instance, aromatic sp^2 C−H bond cleavage is not reversible under thermolysis conditions, and the meta and para products are formed irreversibly from *σ*-**B**. In other words, the product distribution of **16a**,**b** derived from **2** is kinetic and not thermodynamic in origin. The fact that the meta vs para product ratio is greater than the statistical value of 2:1 suggests that the distribution arises from the relative energies of meta vs para C−H bond scission from the corresponding *π*-arene complexes. This interpretation is consistent with the fact that the CF$_3$ group is known to direct the electrophilic C−H activation of arenium cations to the meta position of the aromatic ring.[22]

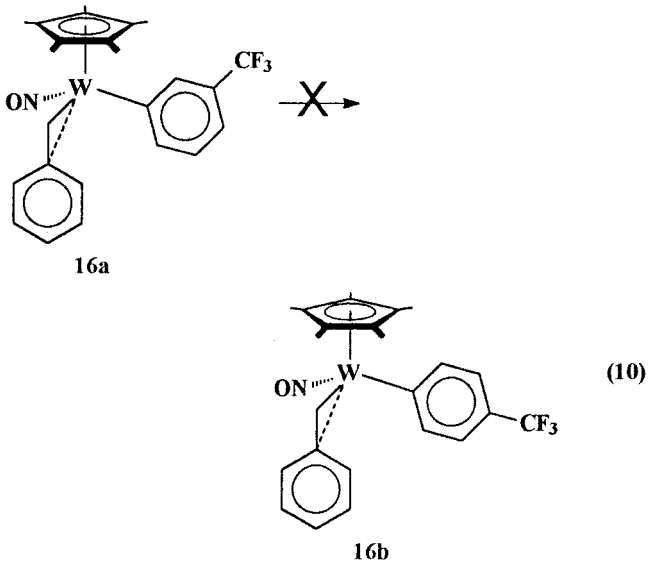

(10)

The last result is in contrast to the results obtained for the activation of this solvent by *σ*-**A**, as well as those obtained for the activation of toluene by *σ*-**B** and *σ*-**A**. One possible explanation for the lack of isomerization of **16a**,**b** is that the electron-withdrawing nature of the CF$_3$ group of the aryl ligand stabilizes the *η*^{2}-benzyl interaction in **16a**,**b** so much that the *η*^{1} conformation of **16a** is not formed in sufficient concentration to permit the reversible sp^2 C−H bond activation and subsequent isomerization under the thermolytic conditions (Scheme 4).

Summary

From the results presented above, it is apparent that there are some similar trends in the activation of arenes

(22) March, J. *Advanced Organic Chemistry: Reactions, Mechanisms and Structure*, 4th ed.; Wiley and Sons: Toronto, ON, 1992; Chapter 11.

by σ-**A** and σ-**B**. For example, for both σ-**A** and σ-**B**, an increased number of methyl groups, or an increase in the number of aromatic sp^2 C−H bonds shielded by these groups, shifts the aryl vs benzyl selectivity toward the benzyl product as well as results in the formation of only one aryl isomer. Likewise, the replacement of a CH_3 group with a CF_3 group shifts the aryl regioisomer distribution toward the meta aryl isomers. However, despite these general trends, it is also apparent that the origins of the observed product selectivities are highly dependent on the nature of the substrate, the nature of the C−H activation products, and the alkylidene complex employed. For example, the origins of the xylene product selectivities are, for the most part, the same as for toluene, but the isomerization of the aryl products to the benzyl products for xylene means that the aryl vs benzyl product distribution is not entirely kinetic in nature. More dramatically, for CF_3 vs CH_3 substituted arenes, the origin of the product distributions is completely different for activations mediated by σ-**A** vs σ-**B**. In short, there is not a singular explanation of the observed chemistry that can be consistently applied to all arene substrates and the two reactive alkylidene species. This fact contrasts with research conducted on other organometallic C−H activation systems for which consistent correlations between the hydrocarbon substrate, the observed product selectivities, and the nature of the reactive metal complex have been discovered.[23]

Experimental Section

General Methods. All reactions and subsequent manipulations involving organometallic reagents were performed under anaerobic and anhydrous conditions under either high vacuum or an atmosphere of prepurified argon or dinitrogen. Purification of inert gases was achieved by passing them first through a column containing MnO and then a column of activated 4 Å molecular sieves. Conventional glovebox and vacuum-line Schlenk techniques were utilized throughout.[24] The gloveboxes utilized were Innovative Technologies LabMaster 100 and MS-130 BG dual-station models equipped with freezers maintained at −30 to −35 °C. Many reactions were performed in a thick-walled bomb, here defined as a glass vessel possessing a Kontes greaseless stopcock and a sidearm inlet for vacuum-line attachment. Small-scale reactions and NMR spectroscopic analyses were conducted in J. Young NMR tubes, which were also equipped with Kontes greaseless stopcocks.

All solvents were dried with appropriate drying agents under N_2 or Ar atmospheres and distilled prior to use, or they were transferred directly under vacuum from the appropriate drying agent. Hydrocarbon solvents, their deuterated analogues, and diethyl ether were dried and distilled from Na or Na/benzophenone ketyl. Tetrahydrofuran was distilled from molten potassium, dichloromethane and chloroform were distilled from calcium hydride, and α,α,α-trifluorotoluene was distilled from P_2O_5.

All IR spectra were recorded on an ATI Mattson Genesis Series FT-IR spectrometer of samples prepared as Nujol mulls sandwiched between NaCl plates. All NMR spectra were recorded at room temperature unless otherwise noted on Bruker AC-200, Bruker AV-300, Bruker AV-400, Bruker WH-400, Bruker AMX-500, or Varian XL-300 instruments. All chemical shifts are reported in ppm, and all coupling constants are reported in Hz. ^{1}H NMR spectra are referenced to the residual protio-isotopomer present in a particular solvent. ^{2}H{^{1}H} NMR (C_6H_6) spectra are referenced to residual C_6H_5D (7.15 ppm), ^{13}C NMR spectra are referenced to the natural abundance carbon signal of the solvent employed, and ^{19}F spectra are referenced to external CF_3COOH (0.0 ppm). Where appropriate, ^{1}H−^{1}H COSY, ^{1}H−^{1}H NOEDS, ^{1}H−^{13}C HMQC, ^{13}C APT, homonuclear decoupling, and gated ^{13}C{^{1}H} experiments were performed to correlate and assign ^{1}H and ^{13}C signals. Ms. M. T. Austria, Ms. L. K. Darge, and Dr. N. Burlinson of the UBC Department of Chemistry NMR facilities assisted in recording some of the spectra. Low-resolution mass spectra (EI, 70 eV) were recorded by the staff of the UBC Chemistry Mass Spectrometry Laboratory on a Kratos MS50 spectrometer utilizing the direct-insertion sample introduction method. All elemental analyses were performed by Mr. P. Borda in the Department of Chemistry at UBC.

Reagents. The $R_2Mg{\cdot}x$(dioxane) (R = CH_2CMe_3, $CH_2C_6H_5$, $CH_2C_6H_4$-3-Me) alkylating reagents[20] and the complexes Cp*W(NO)(CH_2CMe_3)$_2$ (**1**) and Cp*W(NO)($CH_2C_6H_5$)(CH_2CMe_3) (**2**) were prepared according to published procedures.[9,18] Cp*W(NO)($CH_2C_6H_5$)Cl was prepared by the published procedure,[16] except that a stoichiometric amount of 1.0 M HCl in Et_2O rather than an atmosphere of HCl gas was used to effect protonolysis. Cp*W(NO)($CH_2C_6H_5$)($CH_2C_6H_4$-3-Me) (**4**) was prepared from Cp*W(NO)($CH_2C_6H_5$)Cl in a manner similar to that employed for **2**, with pertinent synthetic and characterization details being presented below.

General Comments on Thermolyses of 1 and 2. The preparations of new compounds via the thermolysis of **1** and **2** were conducted in the same manner. A bomb was charged with 75−100 mg of **1** or **2**, a magnetic stir-bar, and 4−5 mL of solvent, the latter being either pipetted directly into the reaction vessel from a storage bomb in a glovebox or vacuum transferred onto the powder on a vacuum line. The sealed bomb was then heated for 40 h in an oil bath set at 70 ± 2 °C, and its contents were stirred. During this time the color of the solution remained either essentially unchanged (deep red-orange) or lightened to an orange or yellow color, depending on the solvent employed. The bomb was then removed from the bath, and the solvent was removed in vacuo. The resulting residue was dissolved in a suitable NMR solvent, and the desired NMR spectral data were obtained. The NMR solvent was then removed under reduced pressure, and the residue was redissolved in an appropriate solvent or solvent mixture for recrystallization. The solution was filtered through Celite supported on a frit, the filtrate was concentrated to the point of incipient crystallization, and the final mixture was placed in a freezer at −30 to −35 °C. The major product(s) were isolated as crystals from the mother liquor after a suitable period of time. The reported yields are not optimized. Minor products that could not be isolated by crystallization were characterized spectroscopically in the final reaction mixture.

For comparisons of product ratios, the thermolyses of **1** and **2** were repeated side-by-side on small scale (12−15 mg, 1.2−1.5 mL of solvent) in J. Young NMR tubes using a VWR 1160A constant-temperature bath set at 70.0 °C. Average product ratios were obtained from multiple (at least five) integrations of like signals in the ^{1}H NMR spectra of the final reaction mixtures recorded on the same NMR spectrometer. The reported errors are standard errors in the mean and have been adjusted for sample size by multiplication of the appropriate Student *t* factor at the 95% confidence level.[25]

Preparation of Cp*W(NO)($CH_2C_6H_5$)(C_6H_3-3,5-Me_2) (3) and Cp*W(NO)($CH_2C_6H_5$)($CH_2C_6H_4$-3-Me) (4). Compounds **3** and **4** were prepared as a mixture from the thermolysis of **2** in *m*-xylene. Complex **3** was isolated as orange blocks (23 mg, 29% yield) from 3:1 Et_2O/hexanes.

(23) For example, see: (a) Schaller, C. P.; Cummins, C. C.; Wolczanski, P. T. *J. Am. Chem. Soc.* **1996**, *118*, 591−611. (b) Bennett, J. L.; Wolczanski, P. T. *J. Am. Chem. Soc.* **1997**, *119*, 10696−10719. (c) Schaller, C. P.; Wolczanski, P. T. *Inorg. Chem.* **1993**, *32*, 131−144.

(24) Shriver, D. F.; Drezdon, M. A. *The Manipulation of Air-Sensitive Compounds*, 2nd ed.; Wiley-Interscience: New York, 1986.

(25) Harris, D. C. *Quantitative Chemical Analysis*, 2nd ed.; W. H. Freeman and Co.: New York, 1987; pp 44−55.

Complex **3**: IR (cm^{-1}) 1559 (s, ν_{NO}); MS (LREI, *m/z*, probe temperature 150 °C) 545 [P^+, ^{184}W], 515 [$P^+ - NO$]; ^1H NMR (400 MHz, CD_2Cl_2) δ 1.80 (s, 15H, C_5Me_5), 2.06 (s, 6H, Xyl Me), 2.38 (d, $^2J_{HH} = 6.0$, 1H, Bzl CH_{syn}H), 3.31 (d, $^2J_{HH} = 6.0$, 1H, Bzl CH_{anti}H), 6.29 (br s, 2H, Xyl H$_{ortho}$), 6.44 (s, 1H, Xyl H$_{para}$), 6.80 (t, $^3J_{HH} = 7.9$, 2H, Bzl H$_{meta}$), 6.93 (d, $^3J_{HH} = 7.1$, 2H, Bzl H$_{ortho}$), 7.34 (t, $^3J_{HH} = 7.5$, 1H, Bzl H$_{para}$); $^{13}C\{^1H\}$ NMR (75 MHz, CD_2Cl_2) δ 10.6 (C_5Me_5), 20.7 (Xyl Me), 48.5 (Bzl CH_2), 109.2 (C_5Me_5), 114.8 (Bzl C$_{ipso}$), 126.5, 129.4, 131.8, 135.3, 135.9, 136.7 (Ar C$_{aryl}$), 173.3 (Xyl C$_{ipso}$). Anal. Calcd for $C_{25}H_{31}$NOW: C, 55.06; H, 5.73; N, 2.57. Found: C, 55.10; H, 5.80; N, 2.64.

Complex **4**: ^1H NMR (400 MHz, CD_2Cl_2) δ −0.11 (d, $^2J_{HH} =$ 9.9, 1H, Bzl CH_{syn}H), 1.17 (d, $^2J_{HH} = 7.9$, 1H, Mxl CH_{syn}H), 1.80 (Bzl CH_{anti}H), 1.85 (s, 15H, C_5Me_5), 2.29 (s, 3H, Mxl Me), 2.66 (d, $^2J_{HH} = 7.9$, 1H, Mxl CH_{anti}H), 6.45 (s, 1H, Mxl H$_{ortho}$), 6.63 (d, $^3J_{HH} = 7.5$, 1H, Mxl H$_{ortho}$), 6.85 (d, $^3J_{HH} = 7.5$, 2H, Bzl H$_{ortho}$), 6.95 (t, $^3J_{HH} = 7.5$, 1H, Bzl H$_{para}$), 7.02 (t, $^3J_{,HH} =$ 7.9, 2H, Bzl H$_{meta}$), 7.10 (t, $^3J_{,HH} = 7.5$, 1H, Mxl H$_{meta}$), 7.42 (d, $^3J_{HH} = 7.5$, 1H, Mxl H$_{para}$).

Independent Preparation of 4 via Metathesis. Complex **4** was also prepared by the reaction of Cp*W(NO)($CH_2C_6H_5$)Cl (0.100 g, 0.21 mmol) and (3-Me-$C_6H_4CH_2$)$_2$Mg·*x*(dioxane) (0.037 g, 0.11 mmol) in THF (10 mL). The final crude residue was extracted with 1:1 CH_2Cl_2/hexanes (15 mL), and the extracts were filtered through alumina I (1 × 0.7 cm) supported on a frit. Concentration of the filtrate followed by its storage at −30 °C overnight afforded **4** as red blocks (85 mg, 74%).

Complex **4**: IR (cm^{-1}) 1554 (s, ν_{NO}); MS (LREI, *m/z*, probe temperature 150 °C) 545 [P^+, ^{184}W], 515 [$P^+ - NO$]; $^{13}C\{^1H\}$ NMR (75 MHz, CD_2Cl_2) δ 10.4 (C_5Me_5), 21.2 (Mxl Me), 41.1, 43.8 (CH_2), 108.2 (C_5Me_5), 113.9 (br, Mxl C$_{ipso}$), 124.9, 125.1, 127.9, 129.1, 130.0, 130.9, 133.0, 138.9, (Ar C$_{aryl}$), 142.3 (Bzl C$_{ipso}$); NOEDS (400 MHz, CD_2Cl_2) δ irrad. at 2.66, NOEs at 1.17, 6.45, 6.63. Anal. Calcd for $C_{25}H_{31}$NOW: C, 55.06; H, 5.73; N, 2.57. Found: C, 55.03; H, 5.88; N, 2.59.

Preparation of Cp*W(NO)($CH_2C_6H_5$)(C_6H_3-3,4-Me_2) (5) and Cp*W(NO)($CH_2C_6H_5$)($CH_2C_6H_4$-2-Me) (6). Complexes **5** and **6** were prepared by thermolysis of **2** in *o*-xylene. Complex **5** was isolated as yellow needles (28 mg, 30%) by recrystallization from 3:1 Et_2O/hexanes.

Complex **5**: IR (cm^{-1}) 1549 (s, ν_{NO}); MS (LREI, *m/z*, probe temperature 150 °C) 545 [P^+, ^{184}W], 515 [$P^+ - NO$]; ^1H NMR (400 MHz, CD_2Cl_2) δ 1.80 (s, 15H, C_5Me_5), 2.02 (s, 3H, Xyl Me), 2.08 (s, 3H, Xyl Me), 2.35 (d, $^2J_{HH} = 6.1$, 1H, Bzl CH_{syn}H), 3.31 (d, $^2J_{HH} = 6.1$, 1H, Bzl CH_{anti}H), 6.25 (br s, 1H, Xyl H$_{ortho}$), 6.62 (m, 2H, Xyl H$_{ortho}$, Xyl H$_{meta}$), 6.80 (t, $^3J_{HH} = 7.6$, 2H, Bzl H$_{meta}$), 6.92 (d, $^3J_{HH} = 7.6$, 2H, Bzl H$_{ortho}$), 7.31 (t, $^3J_{HH} = 7.6$, 1H, Bzl H$_{para}$); $^{13}C\{^1H\}$ NMR (75 MHz, CD_2Cl_2) δ 10.7 (C_5Me_5), 18.9, 19.6 (Xyl Me), 48.6 (Bzl CH_2), 109.2 (C_5Me_5), 115.0 (Bzl C$_{ipso}$), 128.5, 129.4, 129.6, 131.9, 132.5, 134.6, 137.1, 139.9 (Ar C$_{aryl}$), 170.3 (Xyl C$_{ipso}$). Anal. Calcd for $C_{25}H_{31}$NOW: C, 55.06; H, 5.73; N, 2.57. Found: C, 54.69; H, 5.55; N, 2.74.

Complex **6**: ^1H NMR (400 MHz, CD_2Cl_2) δ − 0.98 (d, $^2J_{HH}$ = 11.9, 1H, Bzl CH_{syn}H), 1.22 (d, $^2J_{HH}$ = 11.9, 1H, Bzl CH_{anti}H), 1.70 (Oxl CH_{syn}H), 1.85 (s, 15H, C_5Me_5), 1.99 (s, 3H, Oxl Me), 3.23 (d, $^2J_{HH} = 6.1$, 1H, Oxl CH_{anti}H), 5.46 (d, $^3J_{HH} = 7.3$, 1H, Oxl H$_{ortho}$), 6.65 (m, 1H, Oxl H$_{meta}$), 7.15 (d, $^3J_{HH} = 7.5$, 1H, Oxl H$_{meta}$), 7.45 (d, $^3J_{HH} = 7.3$, 2H, Bzl H$_{ortho}$), 7.82 (t, $^3J_{HH} =$ 7.5, 1H, Oxl H$_{para}$), other signals for the benzyl ligand obscured; NOEDS (400 MHz, CD_2Cl_2) δ irrad. at − 0.98, NOE at 7.45.

Preparation of Cp*W(NO)($CH_2C_6H_5$)(C_6H_3-2,5-Me_2) (7) and Cp*W(NO)($CH_2C_6H_5$)($CH_2C_6H_4$-4-Me) (8). Compounds **7** and **8** were prepared by the thermolysis of **2** in *p*-xylene. Complex **7** was subsequently crystallized from 4:1 Et_2O/hexanes as red needles (36 mg, 40% yield).

Complex **7**: IR (cm^{-1}) 1569 (s, ν_{NO}); MS (LREI, *m/z*, probe temperature 150 °C) 545 [P^+, ^{184}W], 515 [$P^+ - NO$]; ^1H NMR (500 MHz, $CDCl_3$) δ 1.81 (s, 15H, C_5Me_5), 1.96 (s, 3H, Xyl Me), 2.50 (br s, 3H, Xyl Me), 2.58 (br s, Bzl CH_{syn}H), 3.35 (d, $^2J_{HH}$ = 5.6, 1H, Bzl CH_{anti}H), 5.34 (br s, 1H, Xyl H$_{ortho}$), 6.50 (d, $^3J_{HH}$ = 7.3, 1H, Xyl H$_{meta/para}$), 6.81 (t, $^3J_{HH} = 7.7$, 2H, Bzl H$_{meta}$), 6.87 (d, $^3J_{HH} = 7.5$, 1H, Xyl H$_{meta/para}$), 7.07 (t, $^3J_{HH} = 7.5$, 1H, Bzl H$_{para}$), 7.11 (d, $^3J_{HH} = 7.7$, 2H, Bzl H$_{ortho}$); $^{13}C\{^1H\}$ NMR (75 MHz, $CDCl_3$) δ 10.4 (C_5Me_5), 19.8, 27.6 (Xyl Me), 52.2 (br, Bzl CH_2), 109.5 (C_5Me_5), 120.0 (br, Bzl C$_{ipso}$), 125.8, 128.2, 128.9, 130.8, 131.6, 134.0, 134.5, 146.5 (Ar C$_{aryl}$), 178.8 (Xyl C$_{ipso}$). Anal. Calcd for $C_{25}H_{31}$NOW: C, 55.06; H, 5.72; N, 2.57. Found: C, 55.24; H, 5.73; N, 2.80.

Complex **8**: ^1H NMR (500 MHz, $CDCl_3$) δ 0.03 (d, $^2J_{HH}$ = 11.4, 1H, Bzl CH_{syn}H), 1.39 (d, $^2J_{HH} = 7.6$, 1H, Pxl CH_{syn}H), 1.54 (d, $^2J_{HH}$ = 11.4, 1H, Bzl CH_{anti}H), 1.80 (s, 15H, C_5Me_5), 2.26 (s, 3H, Pxl Me), 2.86 (d, $^2J_{HH} = 7.6$, 1H, Pxl CH_{anti}H), 6.69 (d, $^3J_{HH} = 7.9$, 2H, Pxl H$_{ortho/meta}$), 6.94 (d, $^3J_{HH} = 7.9$, 2H, Pxl H$_{ortho/meta}$), aromatic signals for the benzyl ligand obscured.

Preparation of Cp*W(NO)($CH_2C_6H_5$)($CH_2C_6H_3$-3,5-Me_2) (9). Complex **9** was prepared as a red microcrystalline powder by the thermolysis of **2** in mesitylene. To obtain single crystals for X-ray crystallographic analysis, the residue was dissolved in 1:1 CH_2Cl_2/hexanes (10 mL), the solution was filtered through Celite supported on a glass frit (1 × 0.7 cm), and the filtrate was concentrated in vacuo to one-third of its original volume. Maintenance of the final solution at −30 °C for several days induced the crystallization of **9** as orange needles (22 mg, 27%): IR (cm^{-1}) 1553 (s, ν_{NO}); MS (LREI, *m/z*, probe temperature 150 °C) 559 [P^+, ^{184}W], 529 [$P^+ - NO$]; ^1H NMR (400 MHz, CD_2Cl_2) δ −0.62 (d, $^2J_{HH} = 11.5$, 1H, Bzl CH_{syn}H), 1.48 (d, $^2J_{HH} = 11.5$, 1H, Bzl CH_{anti}H), 1.54 (d, $^2J_{HH} = 6.6$, 1H, Mes CH_{syn}H), 1.82 (s, 15H, C_5Me_5), 2.27 (s, 6H, Mes Me), 2.92 (d, $^2J_{HH} = 6.6$, 1H, Mes CH_{anti}H), 6.26 (s, 2H, Mes H$_{ortho}$), 6.85 (d, $^3J_{HH} = 7.5$, 2H, Bzl H$_{ortho}$), 6.89 (t, $^3J_{HH} = 7.3$, 1H, Bzl H$_{para}$), 7.00 (t, $^3J_{HH} = 7.5$, 2H, Bzl H$_{meta}$), 7.42 (s, 1H, Mes H$_{para}$); $^{13}C\{^1H\}$ NMR (75 MHz, CD_2Cl_2) δ 10.6 (C_5Me_5), 21.0 (Mes Me), 39.3 (CH_2), 43.8 (CH_2), 108.1 (C_5Me_5), 118.9 (Mes C$_{ipso}$), 123.4, 127.7, 129.8, 130.9, 132.5, 139.5 (Ar C$_{aryl}$), 148.4 (Bzl C$_{ipso}$); NOEDS (400 MHz, CD_2Cl_2) δ irrad. at 2.92, NOEs at 1.54, 6.26; irrad. at 6.26, NOEs at 1.54, 2.27, 2.92. Anal. Calcd for $C_{26}H_{33}$NOW: C, 55.93; H, 5.95; N, 2.50. Found: C, 55.63; H 5.86; N.2.56.

Preparation of Cp*W(NO)(CH_2CMe_3)(C_6H_4-2,5-Me_2) (10), Cp*W(NO)(CH_2CMe_3)($CH_2C_6H_4$-4-Me) (11), Cp*W(NO)-($CH_2C_6H_4$-4-Me)(C_6H_4-2,5-Me_2) (12), and Cp*W(NO)-($CH_2C_6H_4$-4-Me)$_2$ (13). Complexes **10**−**13** were prepared by the thermolysis of **1** in *p*-xylene. After removal of solvent from the final reaction mixture in vacuo, the oily residue remaining was chromatographed on neutral alumina I (∼2 × 0.7 cm) by eluting with hexanes until a purple band developed, and then with 3:1 (v/v) hexanes/Et_2O to elute it. Reducing the volume of the eluate in vacuo, followed by storing it at −30 °C for several days, afforded **10** as mauve rods (26 mg, 33%). A second orange-yellow band was eluted from the alumina column with 2:1 hexanes/Et_2O. This fraction was then stored at −30 °C overnight to induce the deposition of **12** as yellow-orange blocks (29 mg, 33%). The ^1H NMR spectra of **11** and **13** matched those previously reported.[16]

Complex **10**: IR (cm^{-1}) 1538 (s, ν_{NO}); MS (LREI, *m/z*, probe temperature 150 °C) 525 [P^+, ^{184}W]; ^1H NMR (300 MHz, C_6D_6) δ 1.25 (s, 9H, CMe_3), 1.55 (s, 15H, C_5Me_5), 2.6 (v br s, Xyl Me), 6.96 (d, $^3J_{HH} = 7.6$, 1H, Xyl H$_{ortho/meta}$), 7.13 (d, $^3J_{HH} = 7.6$, 1H, Xyl H$_{ortho/meta}$), other signals not observed; ^1H NMR (500 MHz, tol-d_8, 213 K) major rotamer δ −0.98 (d, $^2J_{HH} = 11.5$, 1H, CH_{syn}H), 1.34 (s, 9H, CMe_3), 1.47 (s, 15H, C_5Me_5), 2.20 (s, 3H, Xyl Me), 2.89 (s, 3H, Xyl Me), 4.08 (d, $^2J_{HH} = 11.5$, 1H, CH_{anti}H), 6.54 (s, 1H, Xyl H$_{ortho}$), 6.85 (d, $^3J_{HH} = 7.6$, 1H, Xyl H$_{ortho/meta}$), 7.17 (d, $^3J_{HH} = 7.9$, 1H, Xyl H$_{ortho/meta}$); minor rotamer δ −3.28 (d, $^2J_{HH} = 10.4$, 1H, CH_{syn}H), 1.33 (s, 9H, CMe_3), 1.48 (s, 15H, C_5Me_5), 1.73 (s, 3H, Xyl Me), 2.31 (s, 3H, Xyl Me), 5.02 (d, $^2J_{HH} = 10.4$, 1H, CH_{anti}H), 8.34 (s, 1H, Xyl H$_{ortho}$), 7.04 (d, $^3J_{HH} = 7.4$, 1H, Xyl H$_{ortho/meta}$), 7.21 (d, $^3J_{HH} =$ 7.7, 1H, Xyl H$_{ortho/meta}$); $^{13}C\{^1H\}$ NMR (125 MHz, CD_2Cl_2) major rotamer δ 9.8 (C_5Me_5), 21.0 (Xyl Me), 25.5 (Xyl Me), 33.1

(CMe_3), 40.0 (CMe_3), 110.8 (C_5Me_5), 111.2 (WCH_2), 127.7, 128.1, 129.9, 130.9, 146.0 (Xyl C_{aryl}), 185.6 (Xyl C_{ipso}); minor rotamer δ 10.0 (C_5Me_5), 20.6 (Xyl Me), 27.7 (Xyl Me), 32.7 (CMe_3), 42.2 (CMe_3), 109.5 (C_5Me_5), 127.8, 129.5, 133.2 (Xyl C_{aryl}), 134.7 (CH_2), 136.3, 140.5 (Xyl C_{aryl}), 180.8 (Xyl C_{ipso}). Anal. Calcd for $C_{23}H_{35}NOW$: C, 52.58; H, 6.72; N, 2.67. Found: C, 52.43; H, 6.59; N, 2.52.

Complex **12**: IR (cm^{-1}) 1548 (s, ν_{NO}); MS (LREI, *m/z*, probe temperature 150 °C) 559 [P^+, ^{184}W], 529 [$P^+ - NO$]; ^1H NMR (300 MHz, C_6D_6) δ 1.59 (s, 15H, C_5Me_5), 1.98 (s, 3H, Ar Me), 2.15 (s, 3H, Ar Me), 2.38 (d, $^2J_{HH} = 6.6$, 1H, $CH_{syn}H$), 2.93 (s, 3H, Ar Me), 3.34 (d, $^2J_{HH} = 6.6$, 1H, $CH_{anti}H$), 5.34 (br s, 1H, Xyl H), 6.34 (d, $^3J_{HH} = 7.8$, 2H, Pxl H), 6.67 (d, $^3J_{HH} = 7.5$, 1H, Xyl H), 6.94 (d, $^3J_{HH} = 7.8$, 2H, Pxl H), 7.04 (d, $^3J_{HH} = 7.5$, 1H, Xyl H); $^{13}C\{^1H\}$ NMR (75 MHz, $CDCl_3$) δ 10.5 (C_5Me_5), 20.5, 21.4, 28.2 (Ar Me), 49.1 (br s, CH_2), 108.9 (C_5Me_5), 111.7 (Pxl C_{ipso}), 124.6, 127.5, 129.8, 129.9, 130.1, 135.2, 135.3, 142.5, 146.9 (Ar C), 180.8 (Xyl C_{ipso}). Anal. Calcd for $C_{26}H_{33}NOW$: C, 55.82; H, 5.95; N, 2.50. Found: C, 55.54; H, 6.06; N, 2.68.

Preparation of Cp*W(NO)(CH_2CMe_3)($CH_2C_6H_3$-3,5-Me_2) (14) and Cp*W(NO)($CH_2C_6H_3$-3,5-Me_2)$_2$ (15). Complexes **14** and **15** were prepared by the thermolysis of **1** in mesitylene. After removal of the organic volatiles from the final reaction mixture under vacuum, the oily brown-yellow residue was redissolved in 4:1 (v/v) hexanes/Et_2O, and the solution was filtered through a short column of neutral alumina I (1 × 0.7 cm). The filtrate was reduced in volume under vacuum and was then stored at −30 °C to induce the deposition of **15** as long orange-yellow needles (26 mg, 43%). Complex **14** was characterized spectroscopically in the final reaction mixture.

Complex **14**: ^1H NMR (400 MHz, $CDCl_3$) δ −2.38 (d, $^2J_{HH} = 13.7$, 1H, Npt $CH_{syn}H$), 0.77 (s, 9H, CMe_3), 1.52 (d, $^2J_{HH} = 13.7$, 1H, Npt $CH_{anti}H$), 1.92 (s, 15H, C_5Me_5), 2.22 (7H, Bzl $CH_{syn}H$, Mes Me), 3.04 (d, $^2J_{HH} = 7.4$, 1H, Bzl $CH_{anti}H$), 6.53 (s, 2H, Mes H_{ortho}), 7.29 (s, 1H, Mes H_{para}).

Complex **15**: IR (cm^{-1}) 1547 (s, ν_{NO}); MS (LREI, *m/z*, probe temperature 150 °C) 587 [P^+, ^{184}W]; ^1H NMR (300 MHz, $CDCl_3$) δ 0.81 (d, $^2J_{HH} = 8.7$, 2H, $CH_{syn}H$), 2.11 (s, 15H, C_5Me_5), 2.46 (d, $^2J_{HH} = 8.7$, 2H, $CH_{anti}H$), 2.50 (s, 12H, Ar Me), 6.68 (s, 4H, Ar H_{ortho}), 7.24 (s, 2H, Ar H_{para}); $^{13}C\{^1H\}$ NMR (75 MHz, $CDCl_3$) δ 10.3 (C_5Me_5), 21.2 (Me), 41.3 ($^1J_{CW} = 66$, CH_2), 107.7 (C_5Me_5), 128.7, 129.1, 132.9 (Ar C), 137.7 (Ar C_{ipso}). Anal. Calcd for $C_{28}H_{37}NOW$: C, 57.25; H, 6.35; N, 2.38. Found: C, 57.14; H, 6.42; N, 2.42.

Preparation of Cp*W(NO)($CH_2C_6H_5$)(C_6H_4-3-CF_3) (16a) and Cp*W(NO)($CH_2C_6H_5$)(C_6H_4-4-CF_3) (16b). Complexes **16a**,**b** were prepared by the thermolysis of **2** in α,α,α-trifluorotoluene and were cocrystallized as a ∼8.3:1 mixture from 2:1 Et_2O/hexanes (43 mg, 39%): IR (cm^{-1}) ν_{NO} 1595; MS (LREI, *m/z*, probe temperature 150 °C) 585 [P^+, ^{184}W], 555 [$P^+ - NO$]; ^1H NMR (400 MHz, C_6D_6) **16a** δ 1.52 (s, 15H, C_5Me_5), 2.09 (d, $^2J_{HH} = 5.8$, 1H, Bzl $CH_{syn}H$), 3.32 (d, $^2J_{HH} = 5.8$, 1H, Bzl $CH_{anti}H$), 6.52 (t, $^3J_{HH} = 7.9$, 2H, Bzl H_{meta}), 6.76 (d, $^3J_{HH} = 7.3$, 2H, Bzl H_{ortho}), 6.92 (t, $^3J_{HH} = 7.6$, 1H, Tol H_{meta}), 7.08 (t, $^3J_{HH} = 7.3$, 1H, Bzl H_{para}), 7.16 (d, $^3J_{HH} = 7.6$, 1H, Tol H_{para}), 8.0 (br d, 1H, Tol H_{ortho}), other H_{ortho} singlet not observed; **16b** δ 1.51 (s, 15H, C_5Me_5), 2.11 (d, $^2J_{HH} = 5.8$, 1H, Bzl $CH_{syn}H$), 3.33 (d, $^2J_{HH} = 5.8$, 1H, Bzl $CH_{anti}H$), 6.44 (t, $^3J_{HH} = 7.9$, 2H, Bzl H_{meta}), 6.73 (d, $^3J_{HH} = 7.3$, 2H, Bzl H_{ortho}), 7.08 (t, $^3J_{HH} = 7.3$, 1H, Bzl H_{para}); 7.21 (d, $^3J_{HH} = 7.6$, 2H, Tol $H_{ortho/meta}$), other doublet obscured; $^{13}C\{^1H\}$ NMR (75 MHz, C_6D_6) **16a** δ 10.3, 10.5 (C_5Me_5), 47.3, 47.4 (CH_2), 108.2, 108.3 (C_5Me_5), 112.7 (Bzl C_{ipso} of **16a**), 112.8 (Bzl C_{ipso} of **16b**), 124.4 (q, $^2J_{CF} = 38$, CCF_3 of **16a**), 118.8, 121.3, 123.1, 129.1, 129.8, 132.5, 132.8, 133.9, 135.6, 135.9, 139.5, 144.9 (Ar C_{aryl}), 168.7 (Tol C_{ipso} of **16a**), 172.2 (Tol C_{ipso} of **16b**), other signals for aryl carbons not observed; ^{19}F NMR (188 MHz, $CDCl_3$) δ 13.98 (**16a**), δ 13.40 (**16b**). Anal. Calcd for $C_{24}H_{26}F_3NOW$: C, 49.25; H, 4.48; N, 2.39. Found: C, 48.86; H, 4.63; N, 2.38.

Preparation of Cp*W(NO)(CH_2CMe_3)(C_6H_4-3-CF_3) (17a) and Cp*W(NO)(CH_2CMe_3)(C_6H_4-4-CF_3) (17b). Complexes **17a**,**b** were prepared by the thermolysis of **1** in α,α,α-trifluorotoluene and were cocrystallized as a ∼11.5:1 mixture from pentane (35 mg, 38%) after filtration through alumina I: IR (cm^{-1}) 1575 (s, ν_{NO}); MS (LREI, *m/z*, probe temperature 150 °C) 565 [P^+, ^{184}W]; ^1H NMR (300 MHz, $CDCl_3$) **17a** δ − 2.58 (d, $^2J_{HH} = 10.8$, 1H, $CH_{syn}H$), 1.12 (s, CMe_3), 1.84 (s, 15H, C_5Me_5), 5.11 (d, $^2J_{HH} = 10.8$, 1H, $CH_{anti}H$), 7.31 (t, $^3J_{HH} = 7.3$, 1H, Tol H_{meta}), 7.38 (d, $^3J_{HH} = 7.2$, 1H, Tol $H_{ortho/para}$), 7.65 (s, 1H, Tol H_{ortho}), 7.77 (d, $^3J_{HH} = 7.4$, 1H, Ar $H_{ortho/meta}$); **17b** δ −2.61 (d, $^2J_{HH} = 10.4$, 1H, $CH_{syn}H$), 1.12 (s, CMe_3), 1.84 (s, 15H, C_5Me_5), 5.13 (d, $^2J_{HH} = 10.4$, 1H, $CH_{anti}H$), 7.41 (d, $^3J_{HH} = 7.4$, 1H, Tol H_{meta}), 7.59 (d, $^3J_{HH} = 7.4$, 1H, Tol $H_{ortho/para}$); $^{13}C\{^1H\}$ NMR (75 MHz, $CDCl_3$) δ 10.2 (C_5Me_5), 33.3 (CMe_3), 42.2 (CMe_3), 111.5 (C_5Me_5), 123.6, 128.8 (m, Ar C_{aryl}), 124.7 (q, $^1J_{CF} = 270$, CF_3 of **17a**), 127.7 (CH_2), 129.3 (q, $^2J_{CF} = 30$, CCF_3 of **17a**), 132.3, 133.0, 137.4, 141.2 (m, Ar C_{aryl}), 178.7 (Tol C_{ipso} of **17a**), 184.4 (Tol C_{ipso} of **17b**), CF_3 and CCF_3 of **17b** not observed; ^{19}F NMR (188 MHz, $CDCl_3$) δ 13.6 (**16a**), δ 13.4 (**16b**). Anal. Calcd for $C_{22}H_{30}F_3NOW$: C, 46.74; H, 5.35; N, 2.48. Found: C, 44.43; H, 5.29; N, 2.48.

Independent Thermolyses of C−H Activation Products. The thermolyses of complexes **3**, **4**, **7**, and **10** in benzene-d_6 were conducted in the same fashion. A J. Young NMR tube was charged with the complex (12−15 mg), solvent (1.2−1.5 mL), and hexamethyldisilane (2 mg, 0.014 mmol) as an integration standard. Thermolyses were conducted in the VWR bath at 70.0 °C, and over the course of 40 h the samples were removed periodically from the heating bath to record ^1H NMR spectra. Thermolyses of these complexes in the parent xylene solvent were conducted on similar scales for 40 h, whereupon the solvent was removed and a ^1H NMR spectrum was recorded for each sample. The thermolysis of **17a**,**b** in benzene-d_6 was also conducted in this fashion, and the ensuing kinetic analysis of the isomerization utilized product ratios determined from ^{19}F NMR spectra recorded at select time intervals. The rate constants and the corresponding equilibrium constant were calculated from the experimental data via nonlinear least-squares analysis of the plot of percent conversion vs time using Origin 5.0 software.[26] The thermolysis of **16a**,**b** in benzene-d_6 was monitored by both ^1H and ^{19}F NMR spectroscopies for a total of 40 h.

X-ray Diffraction Analyses of Complexes 7 and 9. Data collection and structure solutions were conducted at the University of British Columbia by Dr. B. O. Patrick. All measurements were recorded at −93(1) °C on a Rigaku/ADSC CCD area detector using graphite-monochromated Mo Kα radiation. Data sets were corrected for Lorentz and polarization effects. The solid-state structures were solved by direct methods or heavy-atom Patterson methods, expanded using Fourier techniques, and refined by full-matrix least-squares methods. The non-hydrogen atoms were refined anisotropically while the hydrogen atoms were included, but not refined. All calculations were performed using the teXsan crystallographic software package of Molecular Structure Corporation.[27]

Acknowledgment. We are grateful to the Natural Sciences and Engineering Research Council of Canada for support of this work in the form of grants to P.L. and postgraduate scholarships to C.S.A. and E.T. We also thank Dr. B. O. Patrick of this Department for solving the crystal structures of complexes **7** and **9**.

Supporting Information Available: Tables listing crystallographic information, atomic coordinates and B_{eq} values, anisotropic thermal parameters, and intramolecular bond distances, angles, and torsion angles. This material is available free of charge via the Internet at http://pubs.acs.org.

OM011000Q

(26) *Origin 5.0*; Microcal Software Inc., 1991−1997.
(27) *teXsan: Structure Analysis Package;* Molecular Structure Corp.: The Woodlands, TX, 1985 and 1992.